Surface Cooling Causes Accelerated Degradation Compared to Tab Cooling for Lithium-Ion Pouch Cells

Ian A. Hunt, Yan Zhao, Yatish Patel, and J. Offer[z]

Department of Mechanical Engineering, Imperial College London, London, United Kingdom

One of the biggest causes of degradation in lithium-ion batteries is elevated temperature. In this study we explored the effects of cell surface cooling and cell tab cooling, reproducing two typical cooling systems that are used in real-world battery packs. For new cells using slow-rate standardized testing, very little difference in capacity was seen. However, at higher rates, discharging the cell in just 10 minutes, surface cooling led to a loss of useable capacity of 9.2% compared to 1.2% for cell tab cooling. After cycling the cells for 1,000 times, surface cooling resulted in a rate of loss of useable capacity under load three times higher than cell tab cooling. We show that this is due to thermal gradients being perpendicular to the layers for surface cooling leading to higher local currents and faster degradation, but in-plane with the layers for tab cooling leading to more homogenous behavior. Understanding how thermal management systems interact with the operation of batteries is therefore critical in extending their performance. For automotive applications where 80% capacity is considered end-of-life, using tab cooling rather than surface cooling would therefore be equivalent to extending the lifetime of a pack by 3 times, or reducing the lifetime cost by 66%.
 [DOI: 10.1149/2.0361609jes]

Manuscript submitted January 26, 2016; revised manuscript received June 17, 2016. Published July 1, 2016.

Due to their high energy and power densities, Lithium-ion batteries are a very important component of electric vehicles, and their use has increased dramatically in recent years as the uptake of hybrid and electric vehicles has increased.[1–3] One of the major challenges of using lithium-ion batteries in hybrid and electric vehicles is thermal management,[4] which is important in order to manage degradation at an acceptable rate whilst maximizing the performance of the batteries and reducing the risk of thermal runaway.[5–7]

Many studies have shown that increased temperature leads to an increase in the rate of degradation,[4,8–11] therefore the effectiveness of a thermal management system is vital in order to maximize the lifetime performance of the pack. The design of a good thermal management system for a battery pack should consider both the overall temperature of the pack and both intra-cell and internal thermal gradients. Poor design of thermal management systems could be a major contributing factor in increasing degradation rates to unacceptable levels.[12]

There are many different techniques that can be used to thermally manage batteries in hybrid and electric vehicles. It is possible to use either air or liquid as the cooling medium, and both of these can be used in either a direct (with cooling medium in contact with the cell) or indirect way. In addition to this, different areas of the cell can be cooled, namely the surfaces of the cell or the cell tabs.[13,14] In general, systems employing air as the cooling medium are considered to be simpler and cheaper to implement, although the performance is limited especially in applications where there is a high heat generation rate or if the batteries are being operated in a high ambient temperature environment. In general, the thermal properties of liquids enable them to remove heat at a greater rate than air when being used as a cooling medium, and therefore are used in applications where large amounts of heat needs to be removed from the batteries, such as in high-power applications.

In addition to standard cooling techniques, there has been some research looking at more esoteric methods of thermal management. These include taking advantage of the latent heat of vaporization through the use of heat pipes, or using evaporative heat transfer fluids in direct contact with the cells.[15–19] Additionally, solid to liquid phase change materials have been investigated, some employing a slurry of small particles of emulsified paraffin, and some employing carbon sheets impregnated with a phase change material.[20–22]

Degradation of lithium-ion batteries is very complicated, with various interdependent mechanisms contributing to both capacity loss (capacity fade) and increased resistance (power fade). Degradation can occur during storage (calendar ageing) and during operation (cycle life), both of which have a strong dependence on temperature.[23,24] Degradation mechanisms include loss of cyclable lithium, as well as the physical breakdown of the anode and cathode materials, and changes at the interfaces of the electrodes and electrolyte.[9]

Several studies have used a semi-empirical approach to find an Arrhenius relationship between temperature and degradation.[8,25–29] These studies generally treat the cell as a homogeneous system with a single average temperature. Whilst this methodology provides a simple framework for measuring and characterizing degradation in lithium-ion batteries, it has been shown that significant temperature gradients can build up during charging and discharging,[30,31] which are ignored when taking this approach.

Battery pack manufacturers spend a large amount of time and resources designing battery packs and thermal management systems that try to maintain each cell in identical thermal and electrical boundary conditions, however the thermal gradients that can build up within the cells themselves can easily be ignored. Additionally, complex battery management systems (BMS) are employed; with increasingly complex models used to understand the state of charge, state of function, and state of health of each cell in a pack. The BMS then uses this information to make interventions such as de-rating performance, balancing cells or controlling the thermal management system. However if these models treat the cells as lumped thermal masses, and do not take into account variations in temperature during operation, then their effectiveness will be compromized. Additionally, cells are often pre-screened before being assembled into packs in order to group 'similar' cells together to ensure homogenous behavior from each cell in a pack. In a series string of cells, balancing the capacity is most important to maximize pack capacity. For cells in parallel balancing the impedance is most important to minimize current inhomogeneities between cells.

Despite all this, if cells are exposed to different boundary conditions, particularly thermal, then their impedance will change and cause current inhomogeneities, both between the layers within individual cells and between cells in parallel (which is analogous to the layers within a cell). It has been shown that a battery under a temperature gradient behaves differently than a battery at the same average isothermal temperature[32] because of non-uniform impedance. Additionally, there has been some work exploring the effects of temperature gradients on degradation that show that a temperature gradient increases the rate of degradation of lithium-ion batteries.[33]

Previously, a small amount of work has been done looking at different cooling techniques for lithium-ion batteries.[34] This work concluded that temperature gradients limit the performance of the cells, namely the instantaneous discharge power, especially at low mean temperatures. In contrast there have been many studies exploring the effect of temperature on the performance and degradation of

[z]E-mail: Gregory.offer@imperial.ac.uk

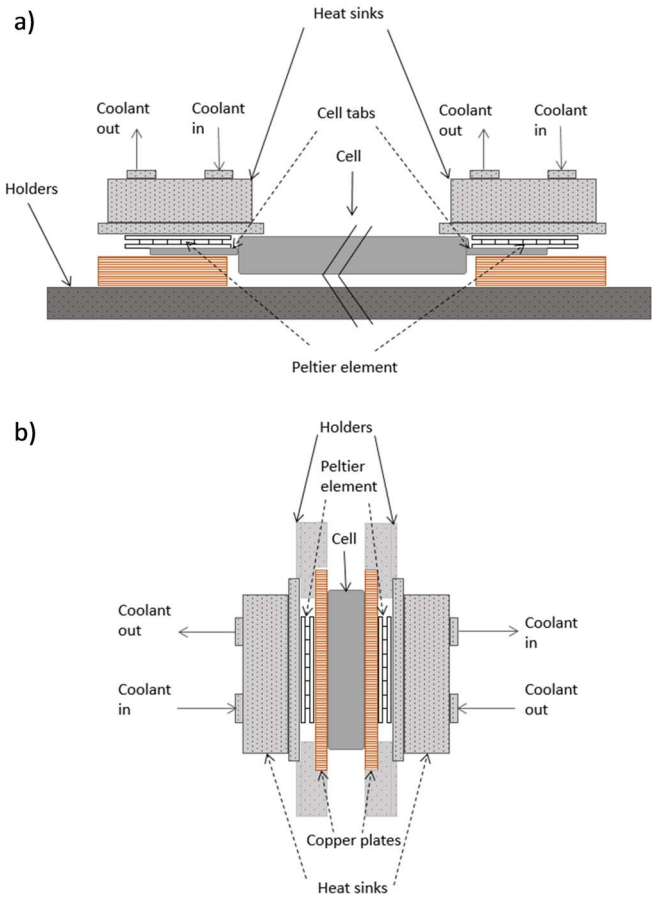

Figure 1. Schematic describing the construction of a) cell tab cooling and b) cell surface cooling rig.

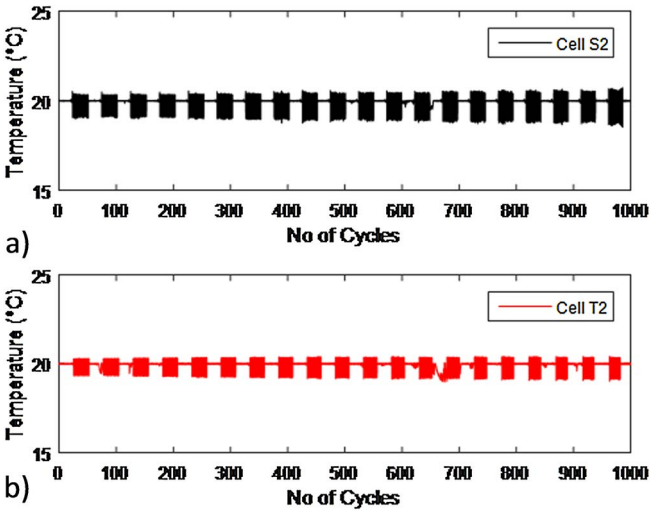

Figure 2. The temperatures of the cells during cycling at; a) Surface cooled cell; b) Tab cooled cell.

lithium-ion batteries, however most of these studies use forced air convection in thermal chambers in order to control the temperature of the cells. These conditions are rarely indicative of the conditions that a cell will experience as part of a battery pack in a real world environment, and more often than not it is assumed that the temperature of the cell is homogenous and the same as the surrounding air.

This study reports for the first time the difference in performance and degradation of cells that are being cooled by different techniques. The techniques were chosen in order to mimic as closely as possible three different thermal boundary conditions that a cell might experience in a battery pack under normal operation, namely cell tab cooling, cell surface cooling and lab-style forced air convection.

Experimental

In this study, the effect on performance and degradation of three different cooling regimes on 5 Ah Kokam pouch cells (model number SLPB11543140H5) were examined. The cooling regimes used were cell tab cooling, cell pouch surface cooling and forced air convection of the entire cell. The cell cooled by forced convection was placed into a Binder incubator set to 20°C with the fan speed set at 100%. The tab cooled and surface cooled cells were placed in custom designed rigs that used Peltier elements to control the temperature of the different surfaces, as shown schematically in Figure 1. Hereafter, the tab cooled cell will be referred to as Cell T, the surface cooled cell as Cell S and the convection cooled cell as Cell C.

The Peltier elements were controlled using a proprietary LabView script utilizing PID control, and powered by two Aim-TTi CPX200DP power supplies. Two battery cyclers were used, a Biologic BCS-815 and a Maccor 4000. Brand new cells from the same batch were used with both battery cyclers. The cells were cycled using the Biologic on run 1 and the Maccor for run 2.

The cells were characterized before cycling. On the Biologic, a 1C charge and discharge was performed, along with electrochemical impedance spectroscopy at 2.7 V and 4.2 V. On the Maccor system, 1C charge and discharges were also conducted, along with a C/20 discharge.

The cells were then cycled using a 6C (30 A) discharge, along with a 2C (10 A) charge. The cells were cycled between 4.2 V and 2.7 V, without employing any constant voltage mode or any rest period between charge and discharge, to ensure that internal temperature gradients did not have time to dissipate. After every 50 cycles, the cells were re-characterized using the same method.

Results and Discussion

Temperature control.—Figure 2 shows the temperature variation measured at the location where temperature was controlled. As shown in Figure 2a, the cell surface temperature was kept within +0.5°C and −1.0°C at the beginning of the degradation cycles. This level of accuracy gradually decreased as the cell degraded with a maximum variation of +0.7°C and −1.2°C measured at cycle 1000. For the tab cooled cell, Figure 2b, the temperature was controlled within +0.2°C and −0.6°C at the beginning of cycling, and +0.3°C and −1.0°C at cycle 1000.

The maximum temperature of the tab cooled cell, measured in the middle of the surface of the cell, was 35.5°C after cycle 1 and 37.8°C after cycle 1000. For the surface cooled cell, the temperature of the tabs was measured giving a maximum of 23.0°C after cycle 1 and 23.2°C after cycle 1000, however due to the electrical connection made at the tabs and therefore additional cooling effect, it is not thought that the measurements for the surface cooled cell are a good indication of the temperature.

Comparison between battery cyclers.—Figures 3b and 3c show the measured capacities for the cells cycled during run 1 and run 2 at 1C and 6C. The results are very comparable, with little variation between the measured capacities at both rates and for all cells. This shows that the results are reliable, and not down to differences such as manufacturing defects within the cells being tested. During run 1, some characterizations were completed at intervals other than 50 cycles due to a number of operational errors and no C/20 discharge was measured. For this reason, the data and results from run 2 will be used from hereon in.

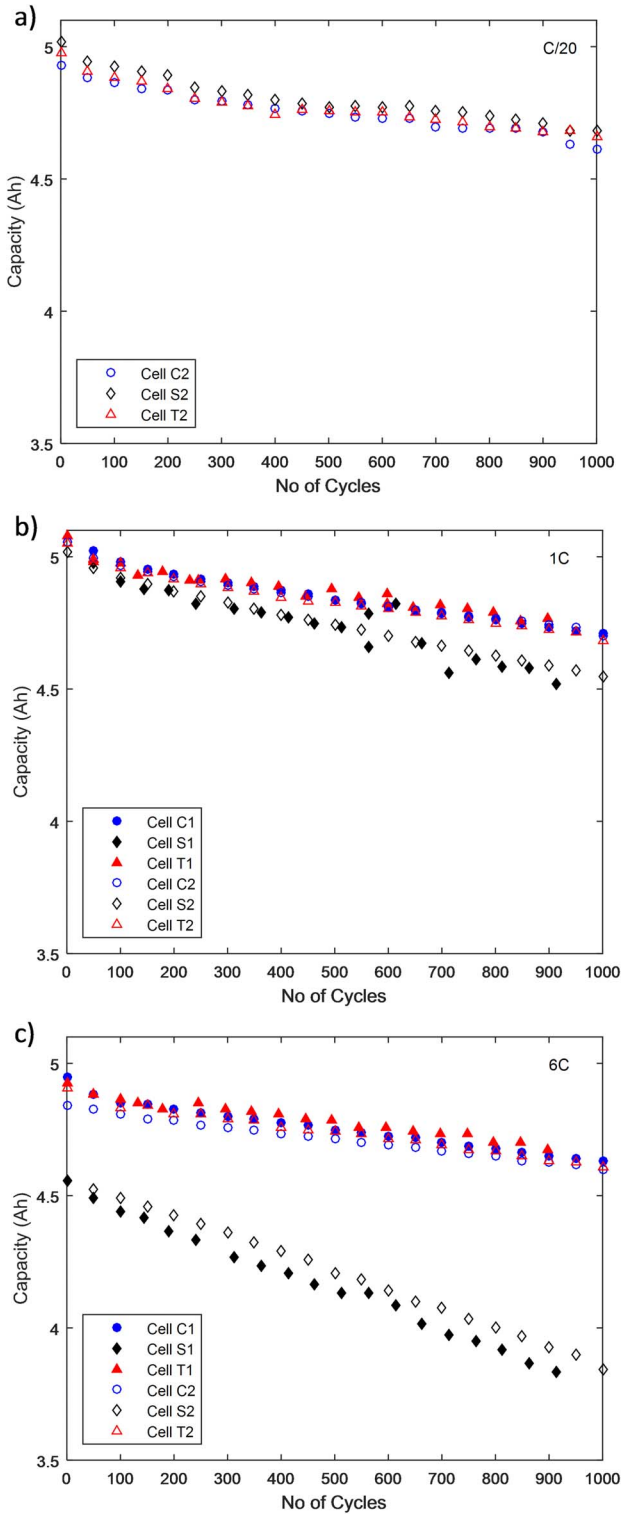

Figure 3. Capacities of cells over 1000 degradation cycles, measured at discharge rate of a) C/20, b) 1C, c) 6C.

Changes in capacity.—Figure 3a shows the capacity at C/20 against number of cycles for the 3 cells tested by the Maccor and the Biologic. The initial capacities of the three cells were 5.02 Ah, 4.97 Ah and 4.93 Ah for Cell S, Cell T, and Cell C respectively. The loss in capacity when measured at this rate was relatively small throughout the course of the tests, and after 1000 cycles the capacities of the cells had dropped to 4.68 Ah, 4.66 Ah and 4.61 Ah. Table I summarizes the capacities at the beginning and after 1000 cycles for the various test rates.

Table I. Capacities at different rates for the beginning and end of cycling.

	Capacity at C/20 (Ah)		Capacity at 1C (Ah)		Capacity at 6C (Ah)	
Cycle Number	0	1000	0	1000	0	1000
Cell S2	5.02	4.68	5.02	4.55	4.56	3.84
Cell T2	4.97	4.66	5.05	4.69	4.91	4.61
Cell C2	4.93	4.61	5.05	4.70	4.84	4.60

It can be seen that the loss of active lithium during the duration of the tests is small, with the drop in capacity between 4.0% and 6.7%.

Whilst very slow discharge tests give a good indication of the capacity fade, i.e. how much active material has been consumed by processes such as SEI formation, they do not give much information regarding how usable the cells are, i.e. power fade. In order to understand this, the capacities at faster discharge rates must be examined. Figures 3b and 3c show the capacity of the cells when measured at 1C and 6C respectively.

At 1C, the initial capacity of all the cells is very similar to the C/20 tests. Additionally, for Cell T and Cell C, the capacities after 1000 cycles are similar between C/20 and 1C tests. However Cell S shows different behavior, with the capacity after 1000 cycles measuring 4.55 Ah, showing a significant decrease in capacity at the higher discharge rate.

At 6C, the initial capacity for all the fresh cells is reduced. This is a reflection of the voltage drop under load triggering the minimum voltage cutoff earlier than at lower C rates. In the case of Cell T and Cell C, the drop in usable capacity is relatively small, with the capacities at 4.91 Ah and 4.84 Ah respectively. In contrast, Cell S's usable capacity is considerably lower at 4.56 Ah. This trend is continued throughout the duration of the test, with the useable capacity of Cell T and Cell C dropping to 4.61 Ah and 4.60 Ah respectively, and usable capacity of Cell S dropping to 3.84 Ah.

Due to the nature of convection cooling, the thermal gradients generated in Cell C will be complex and in multiple directions, and therefore the results for this cell will not be discussed further.

Significance of results.—As shown in Figure 3c, at higher rates of discharge the usable capacity before cycling of Cell S is reduced significantly in comparison to Cell T. This usable capacity is then reduced further as the cell is cycled. In order to understand whether Cell S had degraded more than Cell T, or if the apparent degradation was caused by the same mechanism as the initial drop in usable capacity for a fresh cell, two further tests were carried out in which Cell S and Cell T were swapped over after 1000 cycles and tested in their opposite test rigs (i.e. Cell S was tested in the tab cooling rig and Cell T the surface cooling rig).

The discharge curves at 6C (30 A) can be seen in Figure 4a. When swapped to the surface cooling rig, Cell T loses some of its usable capacity, and Cell S gains some when placed in the tab cooling rig. When comparing the discharge curves of both cells during tab cooling, the voltage curve of Cell S is consistently lower than Cell T, and the final usable capacity is slightly lower at 4.54 Ah compared to 4.61 Ah for Cell T.

A similar trend is seen when comparing both the cells in the surface cooling rig. The voltage of Cell T is higher than that of Cell S, and the usable capacity of Cell T is significantly higher than that of the Cell S at 4.30 Ah compared to 3.84 Ah. Therefore, they are not in the same state, and have degraded differently. The difference is not just an effect of the cooling conditions.

At the beginning of life the lower useable capacity for Cell S suggests that the mean temperature is lower than that of Cell T. It is accepted that higher temperatures lead to faster rates of degradation,

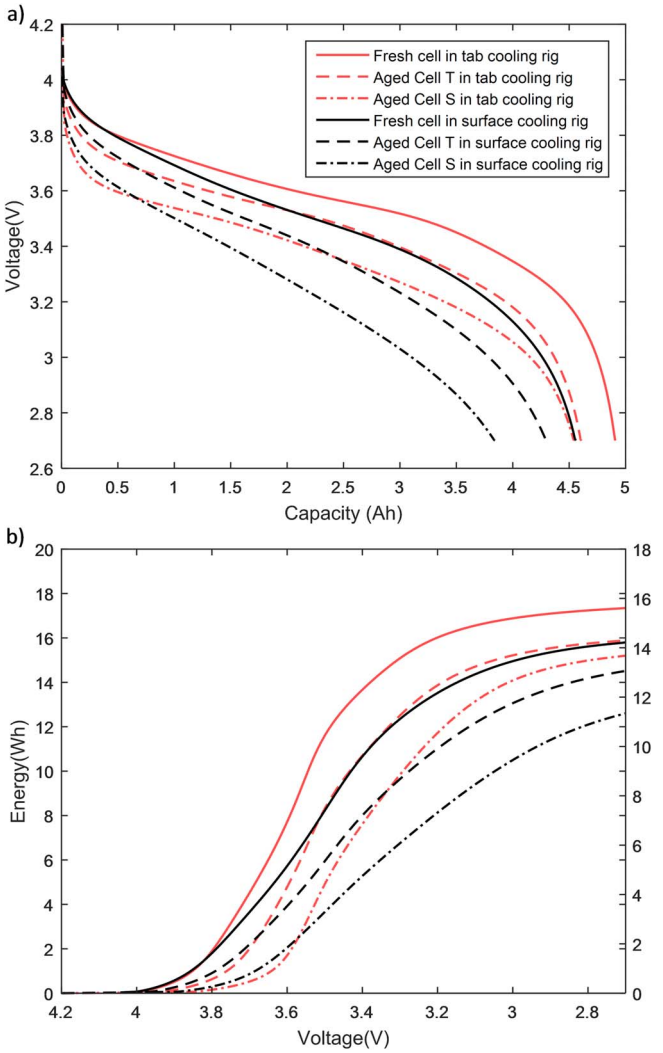

Figure 4. Comparison of the effect of the different cooling methods on the cells after 1000 cycles, showing a) Discharge curves; b) Cumulative energy curves.

and therefore this result cannot be predicted using average temperature alone.

In Figure 4a after 1000 cycles the voltage curves for Cell S are always below that of Cell T, both when both cells are in the surface cooling rig, and when both cells are in the tab cooling rig. This indicates that the cause of the drop in usable capacity under load is an increase in the impedance of the cell. In order to consider the effects of lower usable capacity and increased resistance, the amounts of energy that the cells provided during discharge were examined and these can be seen in Figure 4b. When both cells were discharged in the tab cooling rig, the amount of energy Cell T provided was 15.9 Wh compared to 15.2 Wh for Cell S. When both cells were discharged in the surface cooling rig, the amount of energy that Cell T provided decreased to 14.5 Wh, compared to Cell S which provided 12.6 Wh. This shows that the two effects, the drop in useable capacity caused by the different temperature profiles during surface cooling, and the drop in useable capacity caused by the increased rate of degradation, can be de-coupled and quantified separately.

Electrochemical impedance spectroscopy.—Further characterization using Electrochemical Impedance Spectroscopy (EIS) was conducted every 50 cycles on the cells cycled using the Biologic. Impedance was measured using a 0.2 A amplitude current at frequencies between 1 Hz and 2 kHz, with the cell at 4.2 V and 20°.

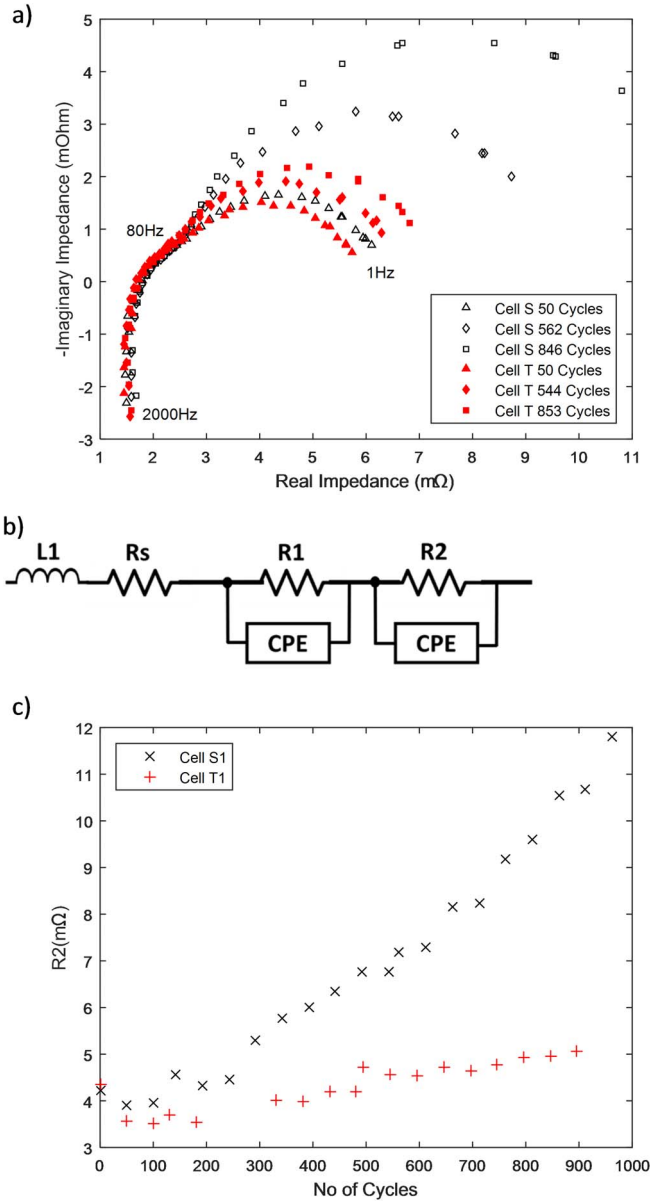

Figure 5. EIS results from the Cell T and Cell S. a) EIS spectra, b) Equivalent circuit model, c) Parameter R2 against number of cycles.

Figure 5a shows a selection of EIS spectra for both Cell S and Cell T and this shows that there is very little change in the high frequency part of the spectra, however the low frequency semi-circle increases with cycling for both cells, but with a significantly larger increase for Cell S.

The spectra were then fitted to the equivalent circuit model shown in Figure 5b using Zview software (Scriber and Assosciates Inc.), and R2, which represents the size of the low-frequency semi-circle is shown in Figure 5c. R2 is commonly attributed to the polarization or charge-transfer resistance of the rate limiting electrode.[35] For both cells, the increase in R2 is relatively linear, however the increase is significantly faster for Cell S than Cell T, which reinforces the conclusion that the surface cooled cell degrades at a faster rate.

Incremental Capacity Analysis (ICA).—Another technique that can be used to diagnose degradation is Incremental Capacity Analysis (ICA).[36,37] Here, dQ/dV, approximated as $\Delta Q/\Delta V$, is plotted against voltage and can be seen in Figure 6. The results were calculated from the C/20 discharges. The data was quite noisy, and therefore was

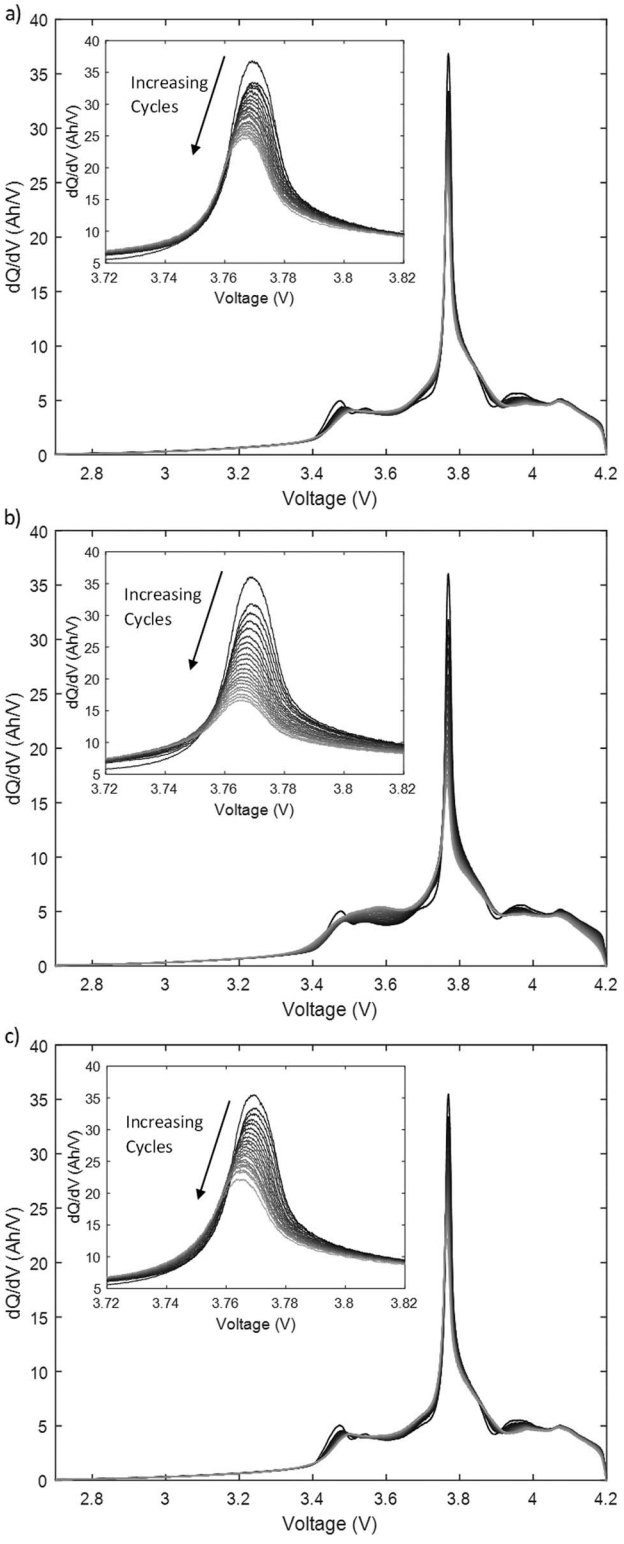

Figure 6. Incremental capacity analysis for a) Cell T, b) Cell S, c) Cell C.

smoothed using Matlab's 'smooth' function (The Mathworks, Inc.). Once the data had been smoothed, the residuals were calculated to check that the mean did not deviate from zero in order to ensure that no artefacts were introduced by the smoothing process. In Figure 6, the lines get lighter as the number of cycles increases, and are taken every 50 cycles.

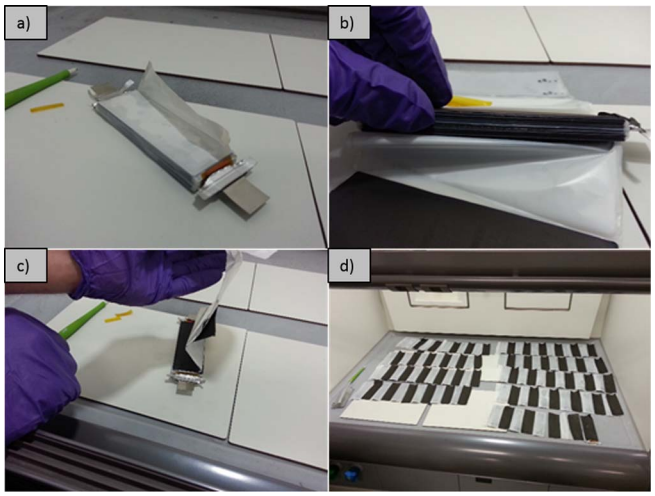

Figure 7. Images of a cell during disassembly; a) Pouch material removed, b) Layers from the side, c) Concertinaed construction of the cell, d) All layers laid out on a bench.

All three sets of data have similar characteristics with a large peak at around 3.75 V and smaller peaks at around 3.5 V and 3.95 V. Figure 6 also includes a close-up of the top of the peak at 3.75 V for each cell. Large peaks on a dQ/dV plot indicate phase equilibria, and it can be seen quite clearly that the peak for the Cell S moves significantly more than the peaks for the Cell T and Cell C. For the fresh cells, the amplitudes of the peaks are quite similar at 36.62, 36.00 and 35.53 Ah/V for Cell T, Cell S and Cell C respectively. However, in the same order, the final magnitudes are 24.63, 16.61 and 22.22 Ah/V. This is a significant change, and indicates that Cell S has degraded differently to Cell T and Cell C.

Further analysis.—In order further analyze the results, it was important to understand how these cells are constructed and their thermal properties. A fresh cell was discharged to 2 V and then taken apart in a fume cupboard using a non-conducting ceramic scalpel. Figure 7 shows that the cells are constructed from alternating layers of anodes and cathodes, separated by a continuous concertinaed separator membrane. The current collectors are coated on both sides by electrode material, apart from the first and last collectors, which are coated only on the side facing inwards. In total, there are 100 anodes and cathodes, on 50 copper (anodic) current collectors and 51 aluminum (cathodic) current collectors.

The thickness of each layer was measured using a calibrated Mitutoyo 293–832 outside micrometer. These are shown in Table II along with the thermal properties taken from Taheri et al.,[38] where the values for the anode, cathode and separator are given whilst these components are wetted with electrolyte.

The thermal resistance, calculated using Equation 1 for both cooling cases, and then using the parallel resistor analogy for tab cooling and series resistor analogy for surface cooling, was found to be 2.4°C/W through the layers (surface cooling), and 3.7°C/W along the length of the cell (tab cooling). These numbers a quite similar

Table II. Thicknesses and thermal properties of cell components.[38]

Component	Thermal Conductivity [$wm^{-1}k^{-1}$]	Thickness [μm]	No. of layers
Copper foil	398	21	50
Aluminium foil	238	21	51
Separator	0.34	24	104
Anode	1.58	38	100
Cathode	1.04	29	100
Casing	238	160	2

– the higher in-plane thermal conductivity is balanced by the longer length (x in Eq. 1) in the tab cooling case. Theoretically, this shows that surface cooling ought to be more effective than tab cooling.

$$R = \frac{x}{A \times k} \quad [1]$$

where x is length in the direction of heat flow, A is area and k is the thermal conductivity.

Therefore, in order to explain these results, the structure of the cell was looked at in more detail. Rather than treating the cell as a single cell, it can be thought of as 100 small cells in parallel with each other. In the surface cooling case, each of these small parallel cells will be at a different temperature depending on how close they are to the edge of the cell. Therefore each layer should have a relatively uniform temperature, but with significant differences in temperature between layers.

During the discharge, the hotter (more central) areas of Cell S will have a lower resistance and therefore provide more current. Heat generation is a function of the current squared, and therefore these areas of the cell will heat up even more, reducing the resistance further and contributing at times to a positive feedback mechanism. Additionally, the heat is generated at the center of the cell; the furthest point from the thermal management system. It has been shown previously that uneven temperatures can lead to inhomogeneous current flow in a parallel string of cells in a battery pack.[39] The construction of these cells is analogous to a parallel string of cells, leading to inhomogeneous current flow through each layer.

This effect can be used to explain why the fresh, uncycled, surface cooled cell exhibits a lower usable capacity at high rates than the tab or convection cooled cells. At the beginning of discharge the central layers of the cell will warm up faster and their impedance will drop and they will be discharged faster, such that by the end of discharge the majority of the current will flow from the outer layers of the cell. These areas are close to the cooling plates, and therefore will be much closer to 20°C than the center of the cell. The colder temperature inhibits solid-state diffusion and increases the polarization resistance, which when coupled to the higher relative current flowing through these areas of the cell, results in the voltage cutoff of 2.7 V being reached much sooner, reducing the usable capacity of the cell.

It has also been show that degradation is highly dependent on current.[5] If the cell is thought of as 100 small cells under a temperature gradient, uneven current will flow and therefore each "small cell" will see periods of higher current flow compared to the average, leading to a localized increased rate of degradation. The increased rate of degradation under thermal gradients has been shown previously.[33]

The same processes will not occur in the case of cell tab cooling, where assuming purely 1-D heat transfer, all the electrode pairs will have the same temperature profile as each other, even though there will be a thermal gradient along the length of the layers. Therefore although this thermal gradient will cause current inhomogeneities during discharge there is no positive feedback between the layers as they all behave and degrade relatively uniformly.

To confirm that at higher rates, the different layers of the surface cooled cell are at different states of charge, the ICA was examined for the fresh cells in the surface cooling and tab cooling rigs before cycling. Therefore the cells are identical except for the thermal boundary conditions during the discharge. Peaks in the ICA curves indicate phase equilibria, and as can be seen in Figure 8 the largest peak is the same for both cells at C/20 but is significantly wider and less intense for the surface cooled cell at higher rates. This indicates that these phase equilibria are happening at different points on the discharge curve for different layers of the surface cooled cell, and therefore take longer and are less intense, indicated by the flattening and widening of the peaks on the graph.

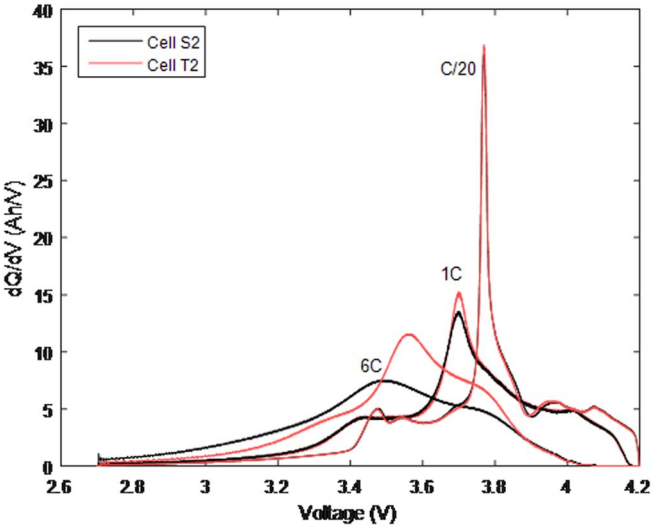

Figure 8. dQdV plots for fresh cells at different rates and with different cooling techniques.

Conclusions

The effect of three different thermal management strategies, cell tab cooling, and cell surface cooling, and forced air convection, on the performance and degradation of lithium-ion batteries was investigated for the first time. 5Ah NCM cathode pouch cells were tested for 1,000 cycles with a 6C discharge and 2C charge between 4.2 V and 2.7 V voltage limits whilst being held at the same target temperature of 20°C. Characterization cycles were performed every 50 cycles to measure capacity fade, power fade and impedance.

All three strategies led to similar reductions of nominal capacity of around 7% measured at C/20. However, at higher rates, discharging the cell in just 10 minutes, surface cooling led to a loss of useable capacity of 9.2% compared to 1.2% for cell tab cooling. After cycling the cells for a 1,000 times, surface cooling resulted in a loss of usable capacity three times higher than cell tab cooling.

This is caused by two effects. Firstly, due to the way the cells are designed, surface cooling causes each parallel internal layer to be at a different temperature and therefore behave differently during discharge, whereas tab cooling causes each parallel layer to behave the same. For surface cooling this leads to non-uniform impedance and therefore non-uniform currents between layers, reducing usable capacity. Secondly, the non-uniform temperatures and currents then cause non-uniform ageing, such that although the same amount of active lithium has been lost in both cases, for surface cooled cells this degradation is distributed unevenly, which causes higher overall cell impedance, i.e. power fade, resulting in voltage cut-offs under load being reached earlier.

Many current battery applications using pouch cells employ surface cooling, taking advantage of the large surface areas of these cells, however this work suggests that this could lead to a significant loss of performance and increased rates of loss of useable capacity under load. Therefore this study shows the vital importance of understanding how cells perform under different thermal conditions before beginning the design of a battery pack and thermal management system.

In a recent MIT technology review,[40] the difficulties of introducing new technologies, such as new electrodes, were discussed including how this can lead to unforeseen problems that may only come to light after years of testing. In contrast, many of the biggest advances in battery technology have come via small incremental changes, often in the way a cell or pack is engineered rather than new cell technologies. Cooling cells via the tabs rather than the surfaces is an example of an improvement to battery pack engineering.

For automotive applications where 80% capacity is considered end-of-life, using tab cooling rather than surface cooling would therefore be equivalent to extending the lifetime of a pack by 3 times, or reducing the lifetime cost by 66%. Nykvist et al.,[41] found that costs

of battery packs declined by around 14% annually between 2007 and 2014. Whilst this reduction was due to a variety of sources, it was found that the main reason was due to input material cost. By significantly reducing the level of degradation, using methods such as those shown in this paper, the costs of battery technology can be reduced further in order to make battery- and hybrid-electric vehicles cost competitive with conventional internal combustion powered vehicles. It is important to note that alongside cell development, battery pack engineering will need to play an important role in making this a reality.

The impact of this work will be most important in high-rate applications such as in the automotive industry. Thermal management systems employing cell tab cooling should be looked at in much more detail, and possible changes to cell construction in terms of dimensions, cell tab location and the number of layers used in a cell should be explored in more detail, either to improve the performance of cell tab cooling thermal management systems, or to reduce the negative consequences of using surface cooling.

Acknowledgments

The authors acknowledge the support from the EPSRC for the Career Acceleration Fellowship for Gregory Offer (EP/I00422X/1) and the FUTURE vehicles project (EP/I038586/1) and Ricardo Ltd for sponsoring the CASE award for Ian Hunt.

References

1. V. Etacheri, R. Marom, R. Elazari, G. Salitra, and D. Aurbach, Challenges in the development of advanced Li-ion batteries: a review, *Energy Environ. Sci.*, **4**, 3243 (2011).
2. A. Du Pasquier, I. Plitz, S. Menocal, and G. Amatucci, A comparative study of Li-ion battery, supercapacitor and nonaqueous asymmetric hybrid devices for automotive applications, *J. Power Sources*, **115**, 171 (2003).
3. B. Scrosati and J. Garche, Lithium batteries: Status, prospects and future, *J. Power Sources*, **195**, 2419 (2010).
4. T. M. Bandhauer, S. Garimella, and T. F. Fuller, A Critical Review of Thermal Issues in Lithium-Ion Batteries, *J. Electrochem. Soc.*, **158**, R1 (2011).
5. G. Ning, B. Haran, and B. N. Popov, Capacity fade study of lithium-ion batteries cycled at high discharge rates, *J. Power Sources*, **117**, 160 (2003).
6. Y. Ye, Y. Shi, N. Cai, J. Lee, and X. He, Electro-thermal modeling and experimental validation for lithium ion battery, *J. Power Sources*, **199**, 227 (2012).
7. N. Tanaka and W. G. Bessler, Numerical investigation of kinetic mechanism for runaway thermo-electrochemistry in lithium-ion cells, *Solid State Ionics*, **262**, 70 (2014).
8. T. Waldmann, M. Wilka, M. Kasper, M. Fleischhammer, and M. Wohlfahrt-Mehrens, Temperature dependent ageing mechanisms in Lithium-ion batteries – A Post-Mortem study, *J. Power Sources*, **262**, 129 (2014).
9. J. Vetter, P. Novák, M. R. Wagner, C. Veit, K.-C. Möller, J. O. Besenhard et al., Ageing mechanisms in lithium-ion batteries, *J. Power Sources*, **147**, 269 (2005).
10. B. A. Johnson and R. E. White, Characterization of commercially available lithium-ion batteries, *J. Power Sources*, **70**, 48 (1998).
11. J. R. Belt, C. D. Ho, T. J. Miller, M. A. Habib, and T. Q. Duong, The effect of temperature on capacity and power in cycled lithium ion batteries, *J. Power Sources*, **142**, 354 (2005).
12. A. Barré, B. Deguilhem, S. Grolleau, M. Gérard, F. Suard, and D. Riu, A review on lithium-ion battery ageing mechanisms and estimations for automotive applications, *J. Power Sources*, **241**, 680 (2013).
13. A. Jarrett and I. Y. Kim, Design optimization of electric vehicle battery cooling plates for thermal performance, *J. Power Sources*, **196**, 10359 (2011).
14. S. J. Stadnick and S. J. Krause, Method and apparatus for transferring heat generated by a battery, US Pat. US6010800 A (2000).
15. H. Hirano, T. Tajima, T. Hasegawa, T. Sekiguchi, and M. Uchino, Boiling Liquid Battery Cooling for Electric Vehicle, in: *2014 IEEE Conf. Expo Transp. Electrif. Asia-Pacific (ITEC Asia-Pacific)*, IEEE, 2014: pp. 1–4.
16. I. Mudawar, D. Bharathan, K. Kelly, and S. Narumanchi, Two-Phase Spray Cooling of Hybrid Vehicle Electronics, *IEEE Trans. Components Packag. Technol.*, **32**, 501 (2009).
17. M.-S. Wu, K. H. Liu, Y.-Y. Wang, and C.-C. Wan, Heat dissipation design for lithium-ion batteries, *J. Power Sources*, **109**, 160 (2002).
18. Z. Rao, S. Wang, M. Wu, Z. Lin, and F. Li, Experimental investigation on thermal management of electric vehicle battery with heat pipe, *Energy Convers. Manag.*, **65**, 92 (2013).
19. Y. Park, S. Jun, S. Kim, and D.-H. Lee, Design optimization of a loop heat pipe to cool a lithium ion battery onboard a military aircraft, *J. Mech. Sci. Technol.*, **24**, 609 (2010).
20. A. Mills, M. Farid, J. R. Selman, and S. Al-Hallaj, Thermal conductivity enhancement of phase change materials using a graphite matrix, *Appl. Therm. Eng.*, **26**, 1652 (2006).
21. S. A. Khateeb, M. M. Farid, J. R. Selman, and S. Al-Hallaj, Design and simulation of a lithium-ion battery with a phase change material thermal management system for an electric scooter, *J. Power Sources*, **128**, 292 (2004).
22. L. Huang, M. Petermann, and C. Doetsch, Evaluation of paraffin/water emulsion as a phase change slurry for cooling applications, *Energy*, **34**, 1145 (2009).
23. R. P. Ramasamy, R. E. White, and B. N. Popov, Calendar life performance of pouch lithium-ion cells, *J. Power Sources*, **141**, 298 (2005).
24. J. Shim, Electrochemical analysis for cycle performance and capacity fading of a lithium-ion battery cycled at elevated temperature, *J. Power Sources*, **112**, 222 (2002).
25. B. Y. Liaw, E. P. Roth, R. G. Jungst, G. Nagasubramanian, H. L. Case, and D. H. Doughty, Correlation of Arrhenius behaviors in power and capacity fades with cell impedance and heat generation in cylindrical lithium-ion cells, *J. Power Sources*, **119-121**, 874 (2003).
26. Y. Zhang and C.-Y. Wang, Cycle-Life Characterization of Automotive Lithium-Ion Batteries with $LiNiO_2$ Cathode, *J. Electrochem. Soc.*, **156**, A527 (2009).
27. L. Lu, X. Han, J. Li, J. Hua, and M. Ouyang, A review on the key issues for lithium-ion battery management in electric vehicles, *J. Power Sources*, **226**, 272 (2013).
28. R. Spotnitz, Simulation of capacity fade in lithium-ion batteries, *J. Power Sources*, **113**, 72 (2003).
29. D. Bernardi, E. Pawlikowski, and J. Newman, A General Energy Balance for Battery Systems, *J. Electrochem. Soc.*, **132**, 5 (1985).
30. C. Forgez, D. Vinh Do, G. Friedrich, M. Morcrette, and C. Delacourt, Thermal modeling of a cylindrical $LiFePO_4$/graphite lithium-ion battery, *J. Power Sources*, **195**, 2961 (2010).
31. R. R. Richardson, P. T. Ireland, and D. A. Howey, Battery internal temperature estimation by combined impedance and surface temperature measurement, *J. Power Sources*, **265**, 254 (2014).
32. Y. Troxler, B. Wu, M. Marinescu, V. Yufit, Y. Patel, A. J. Marquis et al., The effect of thermal gradients on the performance of lithium-ion batteries, *J. Power Sources*, **247**, 1018 (2014).
33. M. Fleckenstein, O. Bohlen, and B. Bäker, Aging effect of temperature gradients in li-ion cells experimental and simulative investigations and the consequences on thermal battery management, *26th Electr. Veh. Symp*, 2012. **1**, 20 (2012).
34. M. Klein, S. Tong, and J. W. Park, The Performance Effects of Edge-Based Heat Transfer on Lithium-Ion Pouch Cells Compared to Face-Based Systems, *SAE Technical Paper 2014-01-1866* (2014).
35. J. Illig, J. P. Schmidt, M. Weiss, A. Weber, and E. Ivers-Tiffée, Understanding the impedance spectrum of 18650 $LiFePO_4$-cells, *J. Power Sources*, **239**, 670 (2013).
36. M. Dubarry, V. Svoboda, R. Hwu, and B. Y. Liaw, Capacity and power fading mechanism identification from a commercial cell evaluation, *J. Power Sources*, **165**, 566 (2007).
37. I. Bloom, A. N. Jansen, D. P. Abraham, J. Knuth, S. A. Jones, V. S. Battaglia et al., Differential voltage analyses of high-power, lithium-ion cells, *J. Power Sources*, **139**, 295 (2005).
38. P. Taheri and M. Bahrami, Temperature Rise in Prismatic Polymer Lithium-Ion Batteries: An Analytic Approach, *SAE Int. J. Passeng. Cars - Electron. Electr. Syst.*, **5**, 164 (2012).
39. B. Wu, V. Yufit, M. Marinescu, G. J. Offer, R. F. Martinez-Botas, and N. P. Brandon, Coupled thermal–electrochemical modelling of uneven heat generation in lithium-ion battery packs, *J. Power Sources.*, **243**, 544 (2013).
40. K. Bull, Why Electric Cars Don't Have Better Batteries, *MIT Technol. Rev.* (2015). http://www.technologyreview.com/review/534866/why-we-dont-have-battery-breakthroughs/ (accessed January 4, 2016).
41. B. Nykvist and M. Nilsson, Rapidly falling costs of battery packs for electric vehicles, *Nat. Clim. Chang.*, **5**, 329 (2015).